Effect of substrate temperature and sputtering pressure on the microstructure and photoluminescence performance of ZnO films by magnetron sputtering

GUANFANG ZHU[a,c,*], PENGPENG GAO[b], YIFAN KANG[a], LIU JING[a], HEBAO YAO[c], CHAO WANG[d]
[a]Institute of Science, Air Force Engineering University, Xi'an710051, China
[b]ESP Research Centre, Xi'an Shiyou University, Xi'an710065, China
[c]Institute of photonics and photon-technology, Northwest University, Xi'an710069, China
[d]Institute of Optics and Precision Mechanics of CAS, Xi'an710119, China

The strong ultraviolet stimulated emission and the weak deep energy level emission was obtained at room temperature. The mechanisms of sputtering pressure impact on growth of ZnO films was also discussed. The low energy tail emission of ultraviolet photoluminescence was caused by the emission of bound exciton. The effect of sputtering pressure on the growth of films were observed. The structural property and photoluminescence performance were studied at different pressures. ZnO films by magnetron sputtering on glass substrates were fabricated with XRD FWHM of only 0.12° exhibiting preferred orientation along c-axis growth at the proper substrate temperature and sputtering pressure.

1. Introduction

Zinc oxide (ZnO) has been exploited in a range of modern optoelctronic applications, specific in ultraviolet laser with the high density storage and fast reaction in the information storage and display taking good use in the submarine detection, ultraviolet communications, optical storage, diagnostic anti-counterfeiting and detection and analysis of instruments and other important application prospects. ZnO was regarded as a wide band-gap semiconductor with an energy band width of 3.37ev and an exciton binding energy of 60mev [1-3], which was easy to obtain strong excitonic emission at room temperature and could be an important material for ultraviolet lasers. ZnO film of resonator structure was obtained by the way of the Molecular Beam Epitaxy (MBE) technology and the ultraviolet stimulated emission of diode-laser was observed at room temperature first time [4-8]. However, the film defects will seriously affect the film's electrical, optical and mechanical properties [9-12]. The defect of films have driven the significant development of the technology of film preparation and detection, etc. Hence, the magnetron sputtering has been use to pare ZnO films due to its high deposition rates, stability and reliability with the technical maturity and low deposition temperature, but the ultraviolet emission performance are affected by elements such as sputtering power and pressure, substrate temperature, oxygen/argon ratio, annealing conditions and etc, in which the substrate temperature and sputtering pressure play a vital role in the structural and optical properties of films. The parameters of the full width at half

maximum (FWHM), luminescent intensity/yellow light and green light ratio play a key role in description of the micro-structure and photoluminescence performance of films. Using the method of magnetron sputtering, Mei has prepared ZnO films onto quartz glass substrate and obtained high-quality crystallization film when the ratio of oxygen to argon was 20/70 and. In this case, the film exhibited preferred orientation along (002) with FWHM of 0.26° [13-14]. Using this method, Zhang also had prepared the ZnO films when the ratio of oxygen to argon was 3/1 with FWHM of 0.30° and it exhibited preferred orientation along c-axis at deposition temperature of 200°C [15-20]. Sang H B [21-24] had also done some works on the pulsed laser deposition of ZnO thin films of light emission.

In this work, ZnO films were prepared on glass substrates with various substrate temperatures via magnetron sputtering at the ultraviolet light/deep level intensity ratio of 17.36 and its XRD FWHM was only 0.12° indicating preferred orientation along c-axis without annealing. And the study of substrate temperature and pressure effect were investigated which was crucial to optical properties of the films. Therefore, the evolution of structural and photoluminescence performance at various substrate temperature and pressure were measured and discussed.

2. Experimental methods

ZnO films were prepared with a magnetron sputtering vacuum machine based on the Atemga JGP560 made by the Shenyang Scientific Instrument Development Center,

Chinese Academy of Sciences on the ZnO target (purity:99.99%). The schematic process of the magnetron sputtering system was schematically illustrated in Fig. 1. Before deposition, the glass substrate have been ultrasonically cleaned in acetone or alcohol for 10 min, then deionized water rinsing repeatedly and drying later, which was put into the vacuum chamber. The base pressure in this system was ~2.5×10-4 Pa and the glass-to-film distance was 15cm with the power of 100w for 1.5h. In the process of sputtering, the argon / oxygen ratio was 2:1 and the bias voltage was 75v. The experiment was divided into two groups: in the first group, at the substrate pressure of 1.9 Pa, the change of the substrate temperature was at temperatures ranging from 25°C, 100°C, 150°C, 200°C, 250°C and 300°C respectively. In the second group, at the substrate temperature of 250°C, the change of the substrate pressure was 1.9Pa, 2.2Pa, 2.6Pa, 3.2Pa and 3.5Pa respectively.
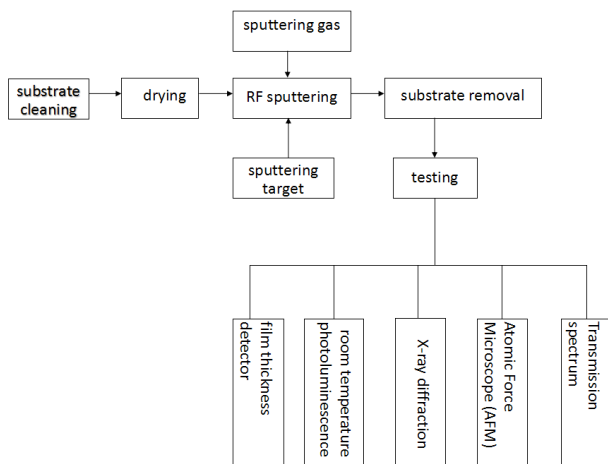
Fig. 1. Schematic diagram of the magnetron sputtering system

The Photoluminescence (PL) spectrum of the films was measured ranging from 220 nm to 700 nm with resolution of 0.5nm, the excitation wavelength of 220 nm and an excitation light source supplied by xenon lamp using the spectrofluorimeter of WGY-10 type. And X-ray diffraction (XRD, CuKα1, λ = 1.54Å) was used to investigate the lattice structure of the films and the atomic force microscope (AFM, SPM9500J3, Japan) was employed to obtain surface morphology information.

3. Result and discussion

3.1. Relations between temperature and film spectrum

The substrate temperatures could directly affect the mobility of the adsorbed atoms on the substrate surface and its re-evaporating and crystallizing. Fig. 2a showed the structure of the prepared samples characterized by XRD at various substrate temperatures. It could be seen that all the

X-ray diffraction (XRD) spectra of all samples represented diffraction peak only around 33.4° with the dominant peak(002) observed in the X-ray diffraction spectra indicating preferred orientation along c-axis. The diffraction peaks growth with good unidirectionality and the diffraction intensity was enhanced from room temperature to 250°C as the substrate temperature increased and its peaks became narrower, indicating that the grain growth, orientation and the crystal quality were improved respectively. The diffraction intensity became weaker at temperature of 300°C due to the softening of the substrate at high temperature which led to the films had a low orientation degree and the diffraction peak intensity and the crystal quality decreased respectively.
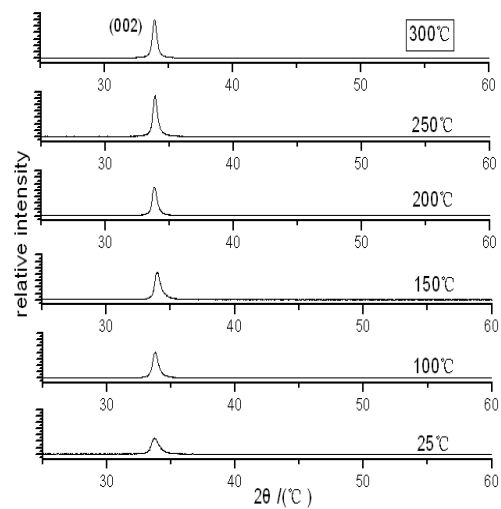
a) Diffraction spectra of ZnO thin films at various substrate temperatures
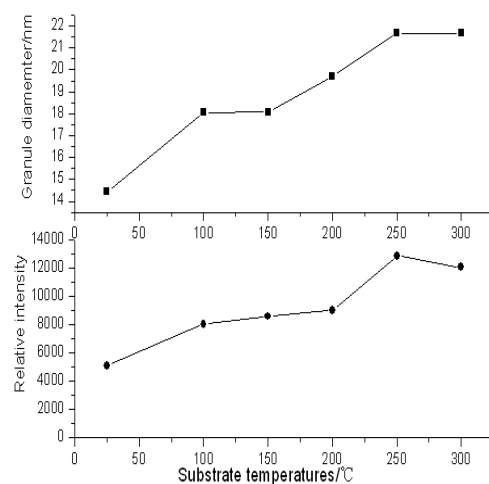
b) Granule diameter and relative intensity of XRD of ZnO thin films at various substrate temperatures.

Fig. 2. Feature of X-ray diffraction spectra, granule diameter and relative intensity of XRD of ZnO thin films at various substrate temperatures

The crystallize size or grain sizes of the thin film samples were calculated using Debye-Scherrer's equation (1) [25-26] are as follows.

$$D = 0.94\lambda/\beta\cos\theta \qquad (1)$$

Where D is the crystallize size, λ is x-ray wavelength (1.5046Å), β is full width at half maximum (FWHM) of the observed peak and θ is the diffraction angle. The average crystallize size was calculated by resolving the highest intensity peak.

The Fig. 2b showed that the crystallization quality of the film was the best at the sputtering temperature of 250°C with good growth of maximum diameter, and the intensity X-ray diffraction achieved maximum simultaneously.
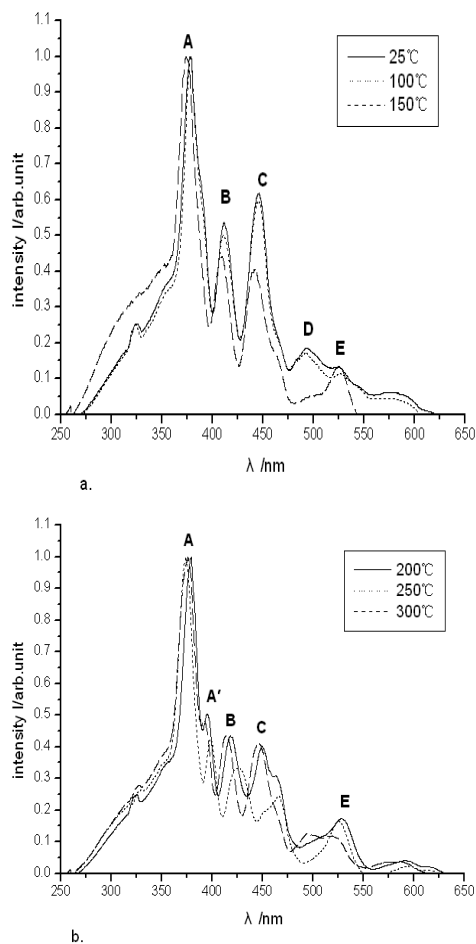
Fig. 3. PL spectrum of ZnO thin films at various substrate temperatures

The photoluminescence (PL) at room temperature were divided into two parts showed in Fig. 3 the near ultraviolet and visible part, among which the the relative intensity of part near ultraviolet with the wavelength ranging from 374 nm to 379.5 nm which was better than that of visible light obviously, and the FWHM was 173mev and the Near-UV emission has been found to be a composite transition from free excitons [27-30]. A peak came from the free exciton compound photoluminescence at the film band-edge and this kind of luminescence could only be found in the films with good crystal-quality and fewer defects [31-34]. According to the results of XRD test, it could be seen that the films had good crystalline quality and excellent luminescence performance without annealing. In addition, the band-edge emission of A' peak (395-398nm) was detected in samples at the substrate temperatures of 200°C, 250°C and 300°C respectively and the difference of the photon energy from A' peak had was 126-129mev compared with the A peak, which was in good agreement with the ZnO acceptor binding energy of 130mev calculated from the hydrogen-like model. Therefore, we thought that the A' peak (395-398 nm) was the results of the emission from bound excitons.

There was a low energy tail in A peak of the sample and the luminescence peaks presented asymmetrical when the substrate temperature was 25°C, 100°C and 150°C respectively, and the beam exciton was superimposed on the low energy direction of the free exciton emission that resulted in the emission A peak was asymmetrical. The superimposed results showed that the free exciton (A peak) shifted towards the samples without superimposition effect of the two kinds of exciton emission at 25°C, 100°C and 150°C respectively and that A peak displayed in asymmetric broadening blue-shifted obviously indicated that the impurities or defects in the film at least. On the other hand, the overheating caused some new defects such as oxygen vacancies and interstitial zinc atoms to form new defect states, which made the bound excitons increased and the bound excitons emitted enhanced led to the A peak red-shifted. From this, the conclusion that both the position of the ultraviolet emission peak and the half-height width (FWHM) of A peak was obviously affected by the emission of bound excitons was obtained finally.

Moreover, the bound excitons were produced by the that the impurity energy level trapped the free excitons. Therefore, the B peak (the ultraviolet light of 409-411nm) and the C peak (the blue light of 441-449 nm) both came from the donor-acceptor pair luminescence (DAP). The luminous intensity as the substrate temperature changing had the same trend with the change of bound exciton emission. The luminous intensity decreased as the increase of the substrate temperature ranging from 0°C to 250°C, accompanied by the disappearance of D peak at 250°C. However, when the temperature exceeded the 250°C, the intensity enhanced again. The reason was that, when the substrate temperature elevated to 300°C, the excessive temperature caused some defects in film structure such as oxgen vacancy, interstitial stom of Zinc. The similarity change trend of the A' peak and C-peak also proved that the the emission of bound excitons was in connection with the donor-acceptor pair luminescence (DAP).
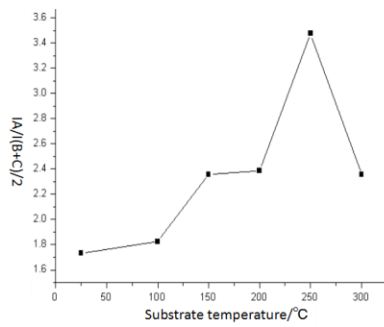
Fig. 4. IA/I(B+C)/2 value of At various substrate temperature/ ℃

Fig. 4 showed the ratio of intensities of UV luminescence to visible light (B and C parts) at various substrate temperatures. As the substrate temperature increased, the relative intensity of UV luminescence showed a clear upward trend and reached the strongest at temperature of 250℃. This was attributed to the fact that the sputtering atoms had sufficient energy to migrate to the lattice site that reduced density of defects such as interstitial atoms or holes and dislocations and possibly of the free excitons captured by the defects in the transition process, made the UV emission enhanced and the luminescence performance optimized, achieving the strong UV-excited emission and weak deep-level emission (green or red light) at room temperature. Meanwhile, the maximum ratio of ultraviolet to green light (528nm) at temperature of 250℃ was 9.3 and the maximum ratio to red light (589nm) was 28. Thereafter, the intensity ratio of UV to visible light (average intensity of B peak plus C peak) began to decrease, which was in agreement with the change between X-ray diffraction (XRD) and substrate temperature. The preferred orientation along c-axis and the photoluminescence (UV) properties achieved the best simultaneously.

Moreover, a weak green peak (525-528 nm), called deep level emission, was produced with the disappearance of D peak when the substrate temperature reached 200°C, 250°C and 300°C respectively showed in Fig. 3(b). There was still theoretical divergence to investigate the emission mechanisms of green-light was proposed by different scholars those who had used different types of electronic transition model so the further research was needed in the future work. Based on the work we had done before, the emission of green light was related to the oxygen vacancy was found. That was to say, as the substrate temperature increased, the green light enhanced. Meanwhile, as the oxygen components decreased, the green light also enhanced indicating that when the temperature increased, the oxygen components might be decreased in our previous tests, so the oxygen atoms were easily resolved from the thin films due to the increase of the substrate temperature, which made the oxygen vacancies increased resulting the green peaks are enhanced.

3.2. Relations between pressure and film spectrum

The crystalline quality and grain orientation of the film were affected by many factors such as working air

pressure the mean free path of particles and the concentration of the oxygen atom on the growth surface. According to the experimental results and discussion above, maintaining the power, argon oxygen flow ratio and other conditions unchanged, in order to obtain better film growth conditions, the sputtering pressure at the substrate temperature of 250℃ was changed in samples under the sputtering pressure of 2.6Pa, 3.2Pa and 3.5Pa respectively, then the films were prepared. The influence of various sputtering pressure on the growth of ZnO thin films was studied, and the best sputtering pressure for film fabrication was found. The atomic force microscope (AFM) surface view and 3D atomic force microscope were depicted in the Fig. 5.

a. 1.9 Pa

b. 2.2 Pa

c.   2.6 Pa

d.   3.2 Pa
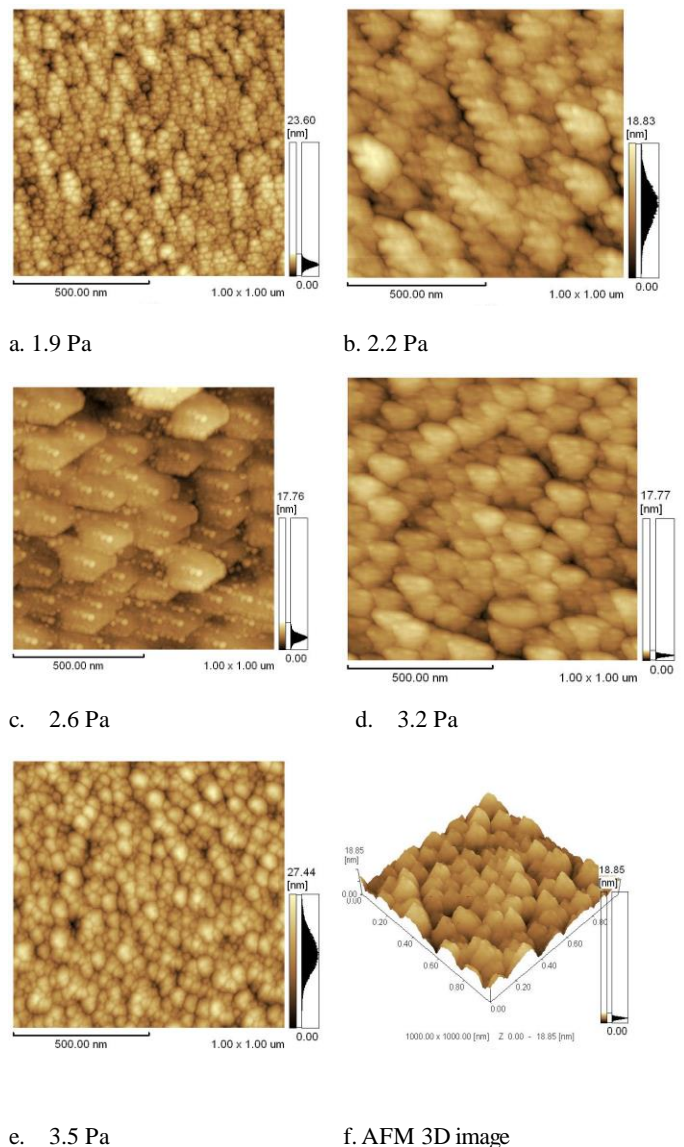
e.   3.5 Pa

f. AFM 3D image

Fig. 5. The AFM ZnO films at various sputtering pressure:a 1.9Pa,b 2.2Pa, c 2.6Pa, d 3.2Pa, e 3.5Pa and f AFM 3D images: atomic force microscope of 3.2 Pa indicting that the film growth was perpendicular to the substrate exhibited preferred orientation along c-axis with columnar growth form

It could be seen that under the low sputtering pressure of 1.9Pa, the grains cluttered on the surface of the ZnO thin film were smaller to display the trend that the grains was likely to merge, but the boundaries between the grains were still obvious in the Fig. 5a And there was no obvious boundaries between the grains under the pressure of 2.2 Pa indicating the larger grains were formed but with the irregular boundary in the Fig. 5b.The grains enhanced bigger with straightening edge under the pressure of 2.6Pa in the Fig. 5c The grains were compact and smoothly covered on the surface in the Fig. 5d under the pressure of 3.2Pa. It could be seen that the ZnO films covered homogeneously on the surface in the Fig. 5f. under the pressure of 3.5Pa and the grains became smaller variously. And the film growth was perpendicular to the substrate showing the "columnar growth" form with highly c-axis preferred growth.

The thin films growth mechanism was discussed carefully. That was, when the pressure was lower than 1.9Pa, the concentration of oxygen atoms in the spaces was not enough to match the amount of zinc atoms sputtered from the target on the film surface, so there was not enough atoms to form a large stable nuclei in a short time. There was only the small stable nucleus formed. Meanwhile, the film was also prone to oxygen vacancies. As the sputtering continues, due to the crystal lattice distortion lager, the grain boundary energy existed there. The higher energy existed in the grain boundary helped to the grains had tendency of transferring spontaneously from the high energy stage to low stage (namely, stable state) and rearrangement to clusters again. Nevertheless, the lower concentration of the atomic on the growth surface was not enough to make the grain boundary disappeared. When the pressure increased to 2.2Pa, the concentration of oxygen atoms in the spaces began to increase and the mismatch between oxygen atoms and zinc atoms decreases, which was favorable to the growth of stable nuclei and the grains had tendency of transferring spontaneously from the high energy stage to low stage (namely, stable state) and rearrangement to clusters again. The binding energy between inter of films was reduced resulting in the nucleus of the new large stable formed at the pressure of 2.2 pa in the Figure 6. As the increase of gas pressure to 2.6Pa, the concentration of oxygen atoms on the film surface further increased, whose concatenation was closer to the one of zinc atoms to meet the requirement of nucleation rate growth, and which was conductive to formation of larger grains in Fig. 5c However, as the atmospheric pressure continued to rise (3.5Pa), the concentration of oxygen atom in the space was greater than the concentration of zinc atoms. The excessive oxygen atoms covering the growth surface hindered the merger between the nuclei and affected the grain growth rustling in the grains became smaller in Fig. 5d and Fig. 5e. Nevertheless, when the pressure increased to 3.2Pa, the surface films tended to smooth, compact and the grain size became comparatively uniform. Based on the analysis above, it was speculated that the oxygen vacancy was related to the

defects of the deep level, so the deep level emission (green emission, namely) of the sample should be the weakest under the gas pressure of 2.6Pa.
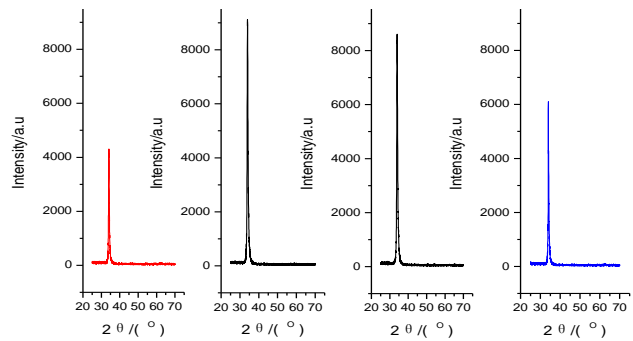
Fig. 6. X-ray diffraction spectra of samples under various sputtering pressures

The results of the diffraction showed that there was only diffraction peaks in (002) in all samples and the peak intensity of the diffraction was weaker under the sputtering pressure of 1.9 Pa which was not shown in the Fig. 6 and the peak of the diffraction was very sharp exhibiting the preferred orientation growth of films in the single orientation in Fig. 6 and the FWHM of the grains became bigger relatively in the Fig. 7.
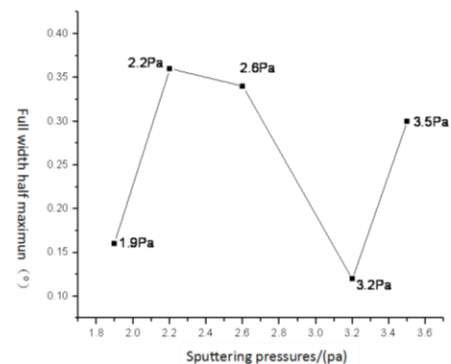
Fig. 7. FWHM of X-ray diffraction under various sputtering pressures (Pa)
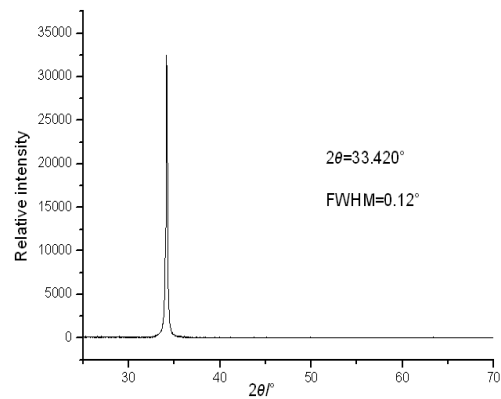
Fig. 8. X-ray diffraction patterns of samples

Using the Debye-Scherrer equation (1), the average crystallite size was 72.31 nm, which was in agreement with the estimated value of the atomic force test results indicating that the test results are reliable. The full width at half maximum(FWHM) was only 0.12° and preferred orientation along c-axis growth was superior to test results reported at home and abroad by method of magnetron sputtering in the Fig. 8. The film was fabricated on the glass substrate in the case of no buffer layers and without annealing.
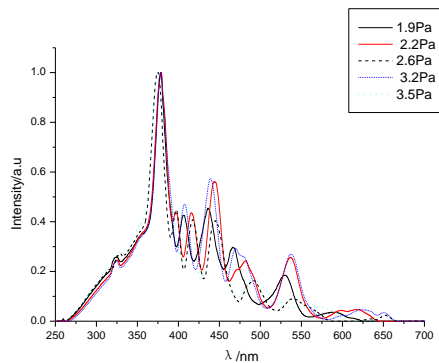
Fig. 9. PL spectra of ZnO thin films at room temperature under various sputtering pressures

Fig. 9 showed the photoluminescence (PL) spectra of ZnO thin films at room temperature under various sputtering pressures. The strong ultraviolet emission PL from the films had been observed at room temperature in all samples indicating the good crystallization quality and few defects. Among which, the UV emission wavelengths of sample C was shortest and the other samples had red-shifts phenomenon (long-wave shift) in different degree compared with UV of c samples as the result of emission superposition from the bound exciton. The reason was that the energy of bound excitons was 130mev slightly lower than that of free exciton and whereas the bound exciton emission was related to the impurity state, so the defect concentration related with the bound exciton was relatively small. On the other hand, the emission of visible light from C-sample was obviously weakened. Namely, the deep-level emission (538nm) was the weakest. The ratio of ultraviolet to deep-level luminescence was 11.76 indicating that the deep-level of defect was the smallest and the grain structure integrity was relative complete. The conclusion was obtained easily that the oxygen vacancies was closely related to the green emission of deep level so that the appropriate oxygen pressure was conducive to reduce the probability of deep level emission of the thin films.

4. Conclusions

In this study, a simple and an effective way was proposed to prepare ZnO films by magnetron sputtering on glass substrates and the films were fabricated at various substrate temperature with XRD FWHM of only 0.12° exhibiting preferred orientation along c-axis growth without annealing. The following conclusions can be made as follows:

1. It was proposed that the low energy tail of the free exciton emission was caused by the excitonic emission superposition of bound excitons, and the ultraviolet light of 395-398nm (A' peak) also came from the bound exciton emission and its emission also affected the position and FWHM of ultraviolet emission peak.

2. The B peak (the ultraviolet light of 409-411nm) and the C peak (the blue light of 441-449nm) both came from the donor-acceptor pair luminescence (DAP).

3. The structure and photoluminescence performance of ZnO films was affected by substrate temperature by the analysis of XRD and PL. The results showed that the orientation along c-axis growth of ZnO became better and the crystallite size increased when the substrate temperature increased from 25°C to 250°C remaining the sputtering pressure of 1.9 Pa constant. The intensity of ultraviolet emission achieved maximum at the substrate temperature of 250°C. The orientation along c-axis growth of ZnO became worse and the crystallite size got smaller at the the substrate temperature of 300°C.

4. The mechanisms of sputtering pressure impact on growth of ZnO films was also discussed. When the pressure was lower than 1.9Pa, the concentration of oxygen atoms in the spaces was not enough to match the amount of zinc atoms sputtered from the target on the film surface, so there was not enough atoms to form a large stable nuclei in a short time. As the sputtering continues, the grain boundary energy existed in the grain boundary helped to the grains had tendency of transferring spontaneously from the high energy stage to low stage (namely, stable state) and rearrangement to clusters again. Under the sputtering pressure of 2.6 Pa, the ZnO grains was the largest with the diameter up to 160nm at the substrate temperature of 250°C. At this moment, the wavelength of ultraviolet emission peak was shortest and the deep level emission was almost disappearing. The ratio of ultraviolet to deep level luminescence was 11.76. Under the the sputtering pressure of 3.2 Pa, the FWHM of XRD peak (002) was 0.12° at the substrate temperature of 250°C and the higher c-axis preferred orientation growth of ZnO was obtained. When the sputtering pressure continued to increase, the orientation along c-axis growth became worse and the crystallite size got smaller.

References

[1] Xu Shurong, Su Zemgmian, Beijing: Chemistry Industry Publishing Company, 2004 (in Chinese).

[2] C. H. Park, C. H. Kim, C. H. Pyun, et al., Journal of Luminescence **s 87 − 89**(5), 1062 (2000).

[3] E. Danielson, M. Devenney, D. M. Giaquinta, et al., Journal of Molecular Structure **470**(1), 229 (1998).

[4] D. M. Bagnall, Y. F. Chen, Z. Zhu, et al., Applied Physics Letters **70**(17), 2230 (1997).

[5] P. Zu, Z. K. Tang, G. K. L. Wong, et al., Solid State Communications **103**(103), 459 (1997).

[6] Z. K. Tang, G. K. L. Wong, P. Yu, et al., Applied Physics Letters **72**(25), 3270 (1998).

[7] P. Zu, Z. K. Tang, G. K. L. Wong, P. Yu, et al., Solid State Communications **103**(8), 459 (1997).

[8] M. Kawasaki, A. Ohtomo, I. Ohkubo, et al., Materials Science & Engineering B **56**(2–3), 239 (1998).

[9] Y. Lin, Z. Ye, L. Chen, et al., Journal of Vacuum Science & Technology **26**(5), 385 (2006).

[10] P. Zu, Z. K. Tang, G. K. L. Wong, et al., Solid State Communications **103**(103), 459 (1997).

[11] J. H. Kim, H. Song, E. K. Kim, Microelectronics Journal **40**(2), 283 (2009).

[12] D. J. Rogers, F. H. Teherani, A. Largeteau, et al., Applied Physics A **88**(1), 49 (2007).

[13] Mei Zengxia, Zhang Xiqiang, et al., Chinese Journal of Luminescence **23**(4), 389 (2002).

[14] Bian Chao, Yao Ning, et al., Vacuum and Cryogenics, **9**(2), 113 (2003).

[15] Zhang Yantao, Li Wancheng, et al., Chinese Journal of Luminescence **24**(1), 73 (2003).

[16] Y. P. Liao, J. H. Zhang, S. X. Li, et al., Physica Status Solidi **207**(8), 1850 (2010).

[17] K. Chen, K. S. Chiang, H. P. Chan, et al., Optical Materials **30**(8), 1244 (2008).

[18] H. Zhu, J. Hüpkes, E. Bunte, et al., Surface & Coatings Technology **205**(3), 773 (2010).

[19] D. H. Zhang, T. L. Yang, J. Ma, et al., Applied Surface Science **158**(1–2), 43 (2000).

[20] X. J. Wang, D. J. Li, H. Q. Tao, et al., Advanced Materials Research **415-417**, 1871 (2011).

[21] H. B. Sang, Y. L. Sang, B. J. Jin, et al., Applied Surface Science **s154–155**, 458 (2000).

[22] J. Elanchezhiyan, K. R. Bae, W. J. Lee, et al., Materials Letters **64**(10), 1190 (2010).

[23] X. Wei, B. Man, C. Xue, et al., Japanese Journal of Applied Physics **45**(11), 8586 (2006).

[24] L. Zhao, J. Lian, Y. Liu, et al., Applied Surface Science **252**(24), 8451 (2006).

[25] A. L. Patterson, Phys. Rev. **56**(10), 978 (1939).

[26] A. W. Burton, K. Ong, T. Rea, et al., Microporous & Mesoporous Materials **117**(s 1–2), 75 (2009).

[27] Tang Xin, Dalian University of Technology, 2008.

[28] S. J. Chen, Y. C. Liu, J. G Ma, et al., Journal of Crystal Growth **240**(3-4), 467 (2002).

[29] D. Zhang, C. Wang, Y. Liu, et al., Optics & Laser Technology **44**(4), 1136 (2012).

[30] T. J. Whang, M. T. Hsieh, J. M. Tsai, et al., Applied Surface Science **257**(22), 9539 (2011).

[31] H. S. Kang, J. S. Kang, J. W. Kim, et al., Journal of Applied Physics **95**(95), 1246 (2004).

[32] O. Lupan, T. Pauporté, L. Chow, et al., Applied Surface Science **256**(6), 1895 (2010).

[33] Zhang Xitian, The Changchun Institute of Optics, Fine Mechanics and Physics (CIOMP), 2002.

[34] H. Nanto, T. Minami, S. Takata, Physica Status Solidi, **65**(65), K131 (1981).

_____

*Corresponding author: zhugf2006@163.com